

Hydrophilic polypropylene microporous membrane for using in a membrane bioreactor system and optimization of preparation conditions by response surface methodology

Hossein Hazrati^{1,2*}, Nader Jahanbakhshi³, Mohammad Rostamizadeh^{1,2}

¹Department of Chemical Engineering, Sahand University of Technology, Tabriz, Iran

²Environmental Engineering Research Center, Sahand University of Technology, Tabriz, Iran

³Young Researchers and Elites Club, North Tehran Branch, Islamic Azad University, Tehran, Iran

Received: 18 July 2017, Accepted: 16 December 2017

ABSTRACT

In this study, the response surface methodology (RSM) based on the central composite design (CCD) was used to optimize the preparation condition of polypropylene-grafted maleic anhydride (PP-g-MA) microporous membrane by thermally-induced phase separation (TIPS) method. A mixture of dibutyl phthalate (DBP) and dioctyl phthalate (DOP) was used as diluent. The effect of polymer composition and quenching bath temperature on the morphology and performance of the fabricated microporous membranes was investigated by using RSM. Analysis of variance (ANOVA) was used to determine which variables and interactions between variables had a significant effect on our responses. The ANOVA revealed that the bath temperature was the most significant variable associated with porosity and pure water flux responses and the polymer concentration was the most significant variable associated with tensile response. The obtained results also showed that with increasing the polymer concentration and decreasing the quenching bath temperature, the membrane porosity and pure water flux decreased, whereas the membrane tensile increased. The regression equations were reasonably validated and used to predict and optimize the performance of PP-g-MA membranes within the limits of the variables. Finally, the maximum responses (flux of 115.6 L/m²h, porosity of 62% and tensile of 1.6 MPa) were obtained under the following conditions: polymer concentration of 28.5 wt% and temperature of 329 K. Further, comparison of laboratory-made and commercial membranes in a membrane bioreactor (MBR) system showed that the rate of membrane fouling was decreased by 4.2 times. **Polyolefins J (2018) 5: 97-109**

Keywords: Response surface methodology; thermally induced phase separation; polypropylene grafted maleic anhydride; membrane; morphology; MBR.

INTRODUCTION

Today, importance of separation processes is undeniable and usually for separation of commercial products, different technologies are used in industries in many aspects. One of these technologies is membrane technology. Indeed, the membrane technology due to its advantages including low cost, low energy consumption, compatibility with environment and high selectivity has gained many attentions in industrial processes dur-

ing the last decades. Based on various criteria such as chemical, mechanical and thermal resistance, adsorption capability, stability, availability and price various materials including polymers, metals, ceramics and gels are used for preparation of membranes [1-5]. Due to versatile properties of polymers, most of membranes are made from polymeric materials. There are many methods for membrane preparation, but most commonly method for polymeric membrane preparation is phase inversion method (solvent evaporation, pre-

* Corresponding Author - E-mail: h.hazrati@sut.ac.ir

precipitation from vapor phase, thermal precipitation and immersion precipitation or diffusion-induced phase inversion). Thermal precipitation (i.e. thermally-induced phase separation (TIPS)) [6-11] and immersion precipitation (solvent/ non-solvent-induced phase separation) [12-16] are two major methods for preparation of phase inversion membranes. In phase inversion method, firstly a homogenous solution is formed, and then by changing composition or temperature, phase separation is occurred. In the immersion precipitation technique, change of composition causes the phase inversion, whereas in the TIPS technique, phase inversion is occurred by changing temperature.

The TIPS technique is applicable to a wide range of polymers which could not be used in the immersion precipitation technique due to their solubility problems, and also in the TIPS technique, there are fewer variables that need to be controlled [17]. So, the TIPS technique due to its advantage over other techniques has been attracted much interest.

Polypropylene (PP) [4, 9, 18-21] is one of polymers that has been commonly used in preparation of TIPS membrane, because it has excellent properties such as low cost, good mechanical properties, thermal stability and chemical resistances [18]. In spite of these outstanding properties, PP membranes suffer from poor wettability and biocompatibility because of their non-polar structure, which limit their application in aqueous solution separation and biomedical purposes. Thus, many efforts have been carried out to improve the surface hydrophilic property of PP.

PP modification has been carried out by different methods such as layer deposition [22], plasma treatment [23], grafting [24, 25], blending [26] and etc. Although, the methods of polymer surface modification such as plasma method are extensive and may be quite complicated. Grafting is one of the frequently used methods to surface modification of PP. Many materials are grafted on PP surface, but maleic anhydride grafted polypropylene (PP-g-MA) may be most important and commercial amphiphilic polymer, which is available in the market [27]. Introducing polar groups of maleic anhydride (MA) to the main chains of PP (Figure 1) improved PP membrane performance.

In spite of conventional methods of experimentation, one of parameters is changed and the others are kept in

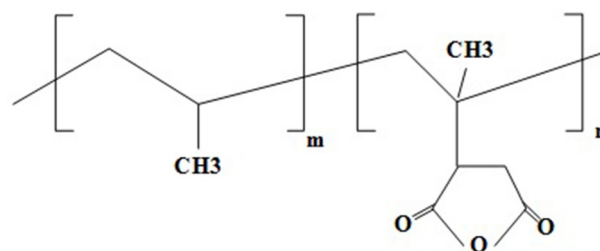


Figure 1. Chemical structure of PP-g-MA.

fixed level, in order to reduce experimental runs and subsequently save time and energy, we applied appropriate response surface methodology (RSM) that all factors are varied together. The RSM explores the relationships between factors and helps us to know how the factors affect response. Also, RSM models have an efficient ability in optimizing the relationship between input design factors and outcome responses. In fact, the main goal in using RSM is to find an optimal condition to achieve best responses. The RSM with using combination of mathematical and statistical techniques is a useful technique for interpretation of the relationship between input factors and response, evaluating the relative significance of affecting factors and optimizing response.

In recent years, RSM has played an important role in different fields for example chemistry and physics, biochemistry and biology, environmental protection and chemical engineering [28, 29]. Nevertheless, few studies have been carried out in application of RSM in membrane field. Ilbeygi et al. [30] used the central composite design (CCD) of the RSM to optimize the content of incorporated additives in sulfonated polyether ether ketone (SPEEK) nanocomposite membrane and predicted its performance. In other investigation, Khayet et al. used RSM to develop predictive models for simulation and optimization of nanofiltration-modified membranes by UV-initiated graft polymerization technique [31]. Idris et al. investigated the composition effect of the aqueous phase used on the interfacial polymerization of thin film composite (TFC) reverse osmosis membrane using RSM [32]. Furthermore, RSM was used to optimize the process parameters for the extraction of platinum (IV) from aqueous solution using emulsion liquid membrane [33].

Various designs of experiments (DOE) are available for developing mathematical modeling. How-

ever, RSM is more promising due to its giving very low average error towards modeling and experimental validation [34, 35].

In our best knowledge, so far there is no work about using RSM to optimize the preparation conditions of PP-g-MA membranes by TIPS technique. In 2014s Saffar et al. [27] prepared hydrophilic microporous membrane by melt extrusion technique by using blending method with PP-g-MA and PP-g-AA. In the mentioned research, no optimization has been done and conventional or classical method has been used to design of experiments. Also, up till now, no attempt has been made on the comparison of a laboratory-made membrane with a commercial membrane in a membrane bioreactor system.

In the current work, microporous flat membranes were prepared through TIPS technique by using PP-g-MA as hydrophilic polymer and mixture of DOP/DBP as diluent. Firstly, the effect of MA on membrane properties was studied. By using RSM approach the effect of initial polymer concentration and quenching bath temperature on membrane performance was also investigated. Finally, optimization of membrane preparation was carried out by the RSM which was used to describe the effects and relationships of the main process independent parameters (initial polymer concentration, quenching bath temperature), to maximize pure water flux. Further, the comparison of laboratory-made and commercial membranes was also done in the MBR system.

EXPERIMENTAL

Experimental for membrane preparation

Polypropylene grafted maleic anhydride (PP-g-MA) with melt flow index ~ 20 g/10 min ($230^\circ\text{C}/2.16\text{kg}$) and a percentage grafting of 1.5% used in this work was purchased from Ariapolymer Company of Iran. Dibutyl phthalate (DBP) and dioctyl phthalate (DOP) mixture (Aekyung Petrochemical Co., Korea) as diluent and ethanol as extractant were used without further purification.

Certain amounts of PP-g-MA and mixture of DBP/DOP were added to a vessel, while the mass ratio of DOP to DBP was kept constant at 1.22. The mixture of

polymer-diluents were heated and stirred at 473 K for 2h until a homogeneous solution was obtained. The homogeneous solution was cast over a preheated glass plate with a thickness of $150\mu\text{m}$, and then submerged in water bath for 10 min. Thermally phase separation was occurred and microporous structure was formed. The diluents were extracted by immersing them into ethanol. Finally, in order to completely remove the diluents and water, the fabricated membranes were dried.

Analytical methods for membrane preparation

Scanning electron microscopy (SEM)

The prepared PP-g-MA membranes were frozen and broken in liquid nitrogen, and then their cross-sections were sputtered with gold-palladium. A KYKY-EM3200 Digital Scanning Electron Microscope (China) with an accelerating voltage of 24 kV was used to observe the membrane morphology.

Porosity measurements

In order to measure the membranes porosity, firstly, the dry weight of membranes were measured and then the membranes were immersed in ethanol for 24 h to become wet, and then immediately weighed after removing ethanol from their surface. The porosity of membranes was calculated according to the following formula [36]:

$$A_k = \frac{(w_2 - w_1)\rho_1}{\rho_1 w_2 + (\rho_2 - \rho_1)w_1} \times 100 \% \quad (1)$$

Where w_1 is the initial membrane weight, w_2 is the immersed membrane weight, and ρ_1 and ρ_2 are the density of PP-g-MA (0.91 g/cm^3) and ethanol (0.8 g/cm^3), respectively.

Pure water flux

Before measuring pure water flux, PP-g-MA membranes were pre-wetted by immersion into ethanol for over 24 h. The membranes with an effective area of 12.56 cm^2 were initially pre-compacted with distilled water at 60 kPa for 20 min. After compaction at 60 kPa, the pure water flux of the membranes was measured at a fixed transmembrane pressure of 48 kPa until the consecutive five recorded values differed by less than 2%. The water flux was calculated using the following equation:

$$J_w = \frac{W}{A \times t} \quad (2)$$

Where J_w , W , A and t are the permeate flux, weight of collected permeate, effective membrane area and time duration of the experiments, respectively. Three trials were performed per each sample and the average values were reported as the permeability of each type of flat sheet membrane.

Mechanical property

The mechanical properties of membranes were measured on the films using a universal testing machine (HIWA 2126, IRAN) at room temperature and according to ASTM D 3039. Each sample was clamped at the both ends with having rectangular geometry of 10 mm wide and 40 mm long, and then was stretched at a cross-head speed of 2mm/min. Three trials were performed per each sample and the average values were reported.

MBR for comparison of laboratory-made and commercial membranes

The dimensions of the membrane bioreactor for this setup were of 60×22×6.5 cm (Figure 2). The effective volume in the reactor was 7L. The aerobic sludge used in the MBR basin was supplied from the activated sludge of the Tabriz Petrochemical Company then adapted with synthetic feed for one month. The synthetic wastewater used in this research was formulated to simulate petrochemical industrial wastewater in terms of chemical oxygen demand (COD).

Analytical methods for MBR

Extracellular polymeric substance (EPS) was measured utilizing the method described by Chang et al. [37]. Protein fraction (EPS_p) was measured by Bradford's method [38], whereas the corresponding polysaccharide fraction (EPS_c) was determined by phenol–sulfuric acid method [39]. Particle size distribution (PSD) was determined by the Fritsch “analysette 22” with a detection range of 0.01–1000 μm.

Experimental design

The RSM was used based on central composite design (CCD) for the statistical design of experiments and data analysis. Central composite design (CCD) is

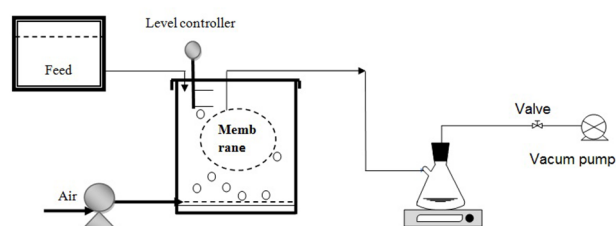


Figure 2. Schematic process flow diagram.

the most common response surface design which is used to:

- Efficiently estimate first- and second-order terms.
- Model a response variable with curvature by adding center and axial points to a previously-run factorial design.

Designs consist of a factorial or fractional factorial design with center points, augmented with a group of axial (or star) points that allow estimation of curvature. Figure 3 represents a classic CCD for 2 factors, whereby:

- Four corners of the square represent the factorial (+/- 1) design points.
- Four star points represent the axial (+/- alpha) design points.
- Replicated center point (coded level 0).

In this study, with using Design Expert Version 9.0.3.1 software, the effect of two independent process variables, initial polymer concentration (A) and quenching bath temperature (B) were investigated and opti-

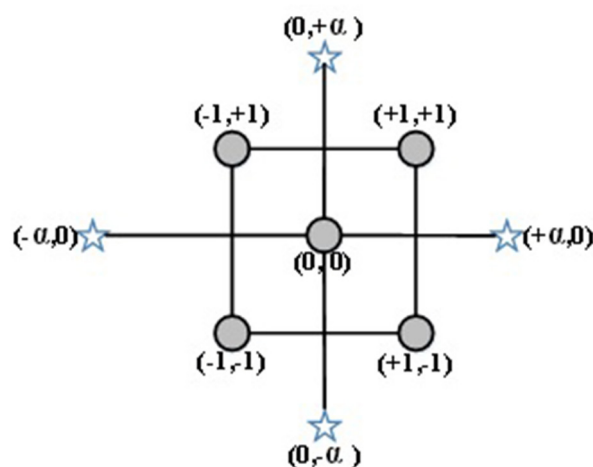


Figure 3. A scheme of a classic central composite design for 2 factors (four corners of the square represent the factorial (+/- 1) design points. Four star points represent the axial (+/- alpha) design points. Replicated center point (coded level 0)).

Table 1. Process variables and their levels.

Factor	variables	Range of actual and coded variables				
		Low axial (-α = -1.41)	Low factorial (-1)	Centre	High factorial (+1)	High axial (+α = +1.41)
A	Polymer concentration	20	21.5	25	28.5	30
B	Bath temperature (K)	303	307	318	329	333

mized using CCD for RSM. Their range and levels are shown in Table 1. The experimental design is generated and summarized in Table 2.

In this study for developing the tensile response, a linear model (Eq. (3)) and for the porosity and pure water flux responses, a quadratic model (Eq. (4)) were used.

$$y = \beta_0 + \beta_1x_1 + \beta_2x_2 + \beta_3x_3 \tag{3}$$

$$y = \beta_0 + \beta_1x_1 + \beta_2x_2 + \beta_3x_3 + \beta_{11}x_1^2 + \beta_{22}x_2^2 + \beta_{33}x_3^2 + \beta_{12}x_1x_2 + \beta_{13}x_1x_3 + \beta_{23}x_2x_3 \tag{4}$$

Where x_1, x_2, x_3 are the independent variables, which influence the response y and the set of β is regression coefficient vector: the constant (β_0), linear ($\beta_1, \beta_2, \beta_3$), interaction ($\beta_{12}, \beta_{13}, \beta_{23}$) and quadratic coefficients ($\beta_{11}, \beta_{22}, \beta_{33}$).

RESULTS AND DISCUSSION

Effect of MA grafting onto PP membrane performance

Initially, it is necessary to confirm that MA is grafted on the surface of the prepared PP-g-MA. Figure 4 con-

firms the good adhesion of MA to the PP matrix. Table 3 also shows that the grafting enhanced the tensile and izod notch impact properties of PP-g-MA samples compared to those of neat PP.

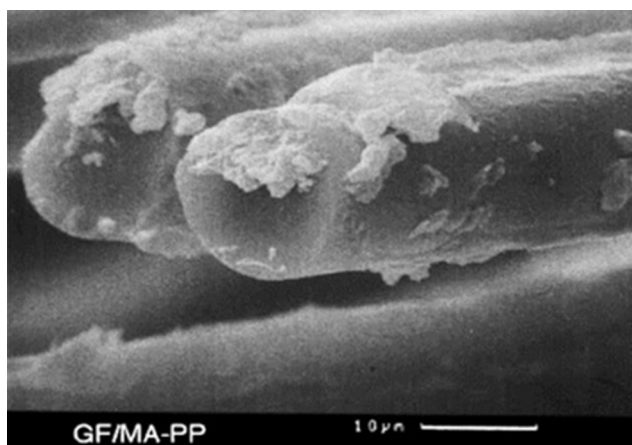
To evaluate the effect of maleic anhydride grafting onto polypropylene membranes, pure water flux for the both PP and PP-g-MA membranes was measured and the results are reported in Table 4. The results indicate a significant influence of maleic anhydride grafting onto polypropylene and its improving effect on the performance of polypropylene membranes. This could be attributed to the presence of polar groups on the membrane surface and the formation of hydrogen bonds with water molecules which enhance the hydrophilicity of PP [27]. This result was also verified by contact angle measurements. These data indicated that the water contact angle decreased from 139° for the nascent membrane to 93° for the modified one (Figure 5).

Analysis of variance

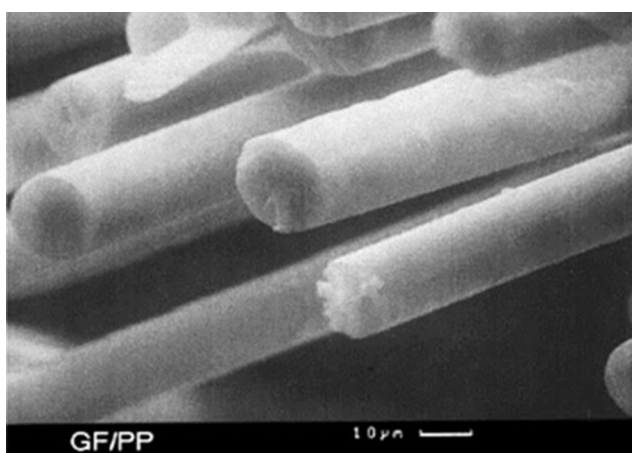
Analysis of variance (ANOVA) was used to determine which variables and interactions between variables significantly affected our responses. In fact, the ANOVA test is the primary step in identifying variables that influencing our response. After doing the ANOVA test,

Table 2. Central composite design and experimental response for PP-g-MA membrane preparation.

Run	Variable A	Variable B	Response 1	Response 2	Response 3
	polymer concentration	temperature	Porosity (%)	Tensile (MPa)	Flux (L/m ² h)
1	30.0	318	54.6±0.7	1.84±0.03	88±3
2	25.0	303	48.2±0.5	1.54±0.01	67±5
3	21.5	307	57.3±1.2	1.07±0.04	101±8
4	20.0	318	66.4±1	0.92±0.04	140±3
5	25.0	333	65.3±0.3	1.28±0.02	134±11
6	25.0	318	57.5±0.5	1.37±0.01	94±2
7	25.0	318	58.3±0.9	1.44±0.06	104±9
8	25.0	318	58.9±0.2	1.47±0.05	109±5
9	25.0	318	56.8±1.2	1.35±0.04	90±4
10	28.5	307	49.7±1.6	1.77±0.01	69±6
11	21.5	329	69.9±0.9	1.00±0.03	160±9
12	25.0	318	57.7±1.5	1.44±0.01	99±8
13	28.5	329	62.0±1.1	1.60±0.02	115±11



(a)



(b)

Figure 4. Morphology of PP-g-MA and PP.

we are able to perform further analysis. These results will help us to focus on what's important, so we can save time and money and can obtain the best performance. In order to get information about the goodness of the fit polynomial model, coefficient of determination (R^2) was used. R^2 -value indicates how well the regression line approximates the real data points. An R^2 of 1 indicates that the regression line perfectly fits the data, so it should be close to one. Significance of variables was evaluated by probability value (P-value). In general, a term that has a P-value less than 0.05 would be considered a significant effect. A P-value greater

Table 4. Effect of MA grafting on PP membrane performance.

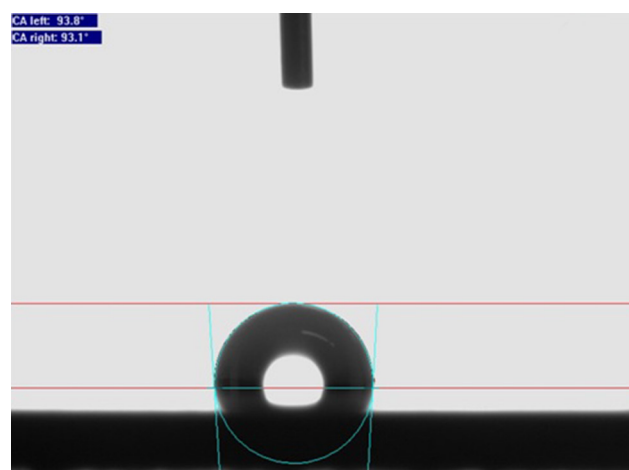
Polymer concentraion (wt%)	Bath temperature (°k)	Pure water flux (L/m ² h)	
		PP	PP-g-MA
25	303	11±1	67±8
25	318	13±1	99±7
25	329	18±2	120±5

Table 3. Effect of MA grafting on tensile and izod impact strength of PP membrane.

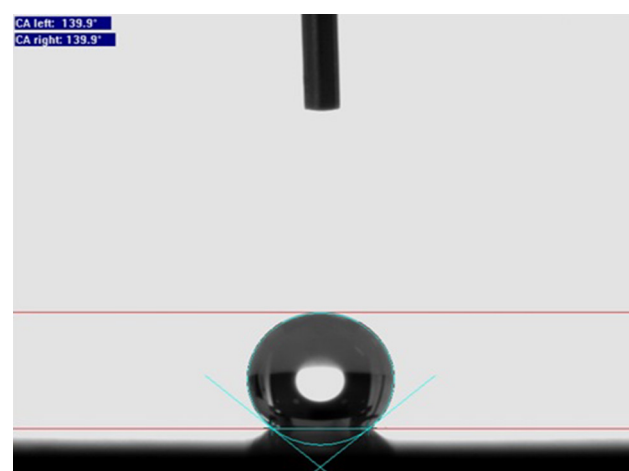
Polymer	Tensile (MPa)	Izod impact strength (KJ/m ²)
PP	53	8
PP-g-MA	81	12

than 0.10 is generally regarded as not significant [29].

Tables 5 and 6 present the ANOVA table for the porosity and tensile, respectively. According to the table 5, the R^2 -value is 0.99 which is satisfactory. It indicates that about 99% of the variability in the data is explained by the model. The adjusted R^2 -value is 0.98, which is acceptable for significance of the model. The adjusted R^2 -value represents the amount of variation that can be explained by the model and is mostly used when comparing models with different



(a)



(b)

Figure 5. Contact angle values for (a) modified and (b) neat membranes.

Table 5. ANOVA of the regression model for porosity.

Source	Sum of Squares	df	Mean Square	F- Value	P-value Prob > F	
Model	450.27	5	90.05	120.92	< 0.0001	significant
A-polymer concentration	129.96	1	129.96	174.50	< 0.0001	
B-temperature	300.69	1	300.69	403.74	< 0.0001	
AB	0.017	1	0.017	0.023	0.8837	
A²	18.02	1	18.02	24.20	0.0017	
B²	0.48	1	0.48	0.64	0.4505	
Residual	5.21	7	0.74			not significant
Lack of Fit	2.68	3	0.89	1.41	0.3624	
Pure Error	2.53	4	0.63			
Cor Total	455.48	12				
R²	0.9886	Adjusted R²	0.9804	Predicted R²	0.9494	

number of terms [32]. The predicted R² of 0.95 is in reasonable agreement with the adjusted R² of 0.98 (i.e. the difference is less than 0.2). The Model F-value of 120.92 implies the model is significant. There is only a 0.01% chance that an F-value this large could occur due to noise. Values of "Prob > F" less than 0.05 indicate model terms are significant. Because of P-values smaller than 0.1 the model terms are significant, so in this case A, B, A² are significant model terms.

The "Lack of Fit F-value" of 1.41 implies the Lack of Fit is not significant relative to the pure error. There is a 36.24% chance that a "Lack of Fit F-value" this large could occur due to noise. Since lack of fit is an undesirable characteristic for a model, non-significant lack of fit is good.

F-value or P-value also is used to compare the order of significance of variables. Variable which has the larger F-value and correspondingly the smaller "Prob > F" value, is more significant variable. Thus, in this study, the significant effects were in the order of B > A > A² > B² > AB for the porosity.

The same procedure is used to analyze other response. The result from ANOVA for tensile response is shown in Table 6. The R², adjusted R² and predicted R² values

are 0.98, 0.97 and 0.96, respectively. The obtained results are acceptable and the model is significant. The model F-value of 203.05 and values of "Prob > F" less than 0.0500 indicate model terms are significant. In this case, A and B are significant model terms.

The "Lack of Fit F-value" of 0.73 implies the Lack of Fit is not significant relative to the pure error as we want the model to fit. There is a 65.12% chance that a "Lack of Fit F-value" this large could occur due to noise. The result from F-value or P-value indicates the polymer concentration variable is more significant than the temperature variable.

Table 7 shows the ANOVA results for pure water flux response. The R², adjusted R² and predicted R² values are 0.97, 0.94 and 0.92, respectively. The model F-value of 42.22 and values of "Prob > F" less than 0.05 indicate model terms are significant. In this case, A, B, A² are significant model terms. This result shows the model is significant and the model has significant effect on the response.

The "Lack of Fit F-value" of 0.24 implies the Lack of Fit is not significant relative to the pure error as we want the model to fit. There is a 86.54% chance that a "Lack of Fit F-value" this large could occur due to

Table 6. ANOVA of the regression model for tensile.

Source	Sum of Squares	df	Mean Square	F- Value	P-value Prob > F	
Model	0.90	2	0.45	203.05	< 0.0001	significant
A-polymer concentration	0.85	1	0.85	384.13	< 0.0001	
B-temperature	0.049	1	0.049	21.97	0.0009	
Residual	0.022	10	2.211E-003			not significant
Lack of Fit	0.012	6	1.929E-003	0.73	0.6512	
Pure Error	0.011	4	2.633E-003			
Cor Total	0.92	12				
R²	0.9760	Adjusted R²	0.9712	Predicted R²	0.9616	

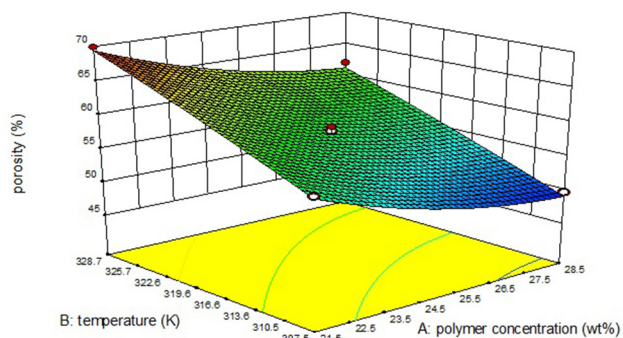


Figure 6. Effects of polymer concentration and bath temperature on membrane porosity.

noise. For pure water flux response, the ranking based on F-value or P-value is as follows:

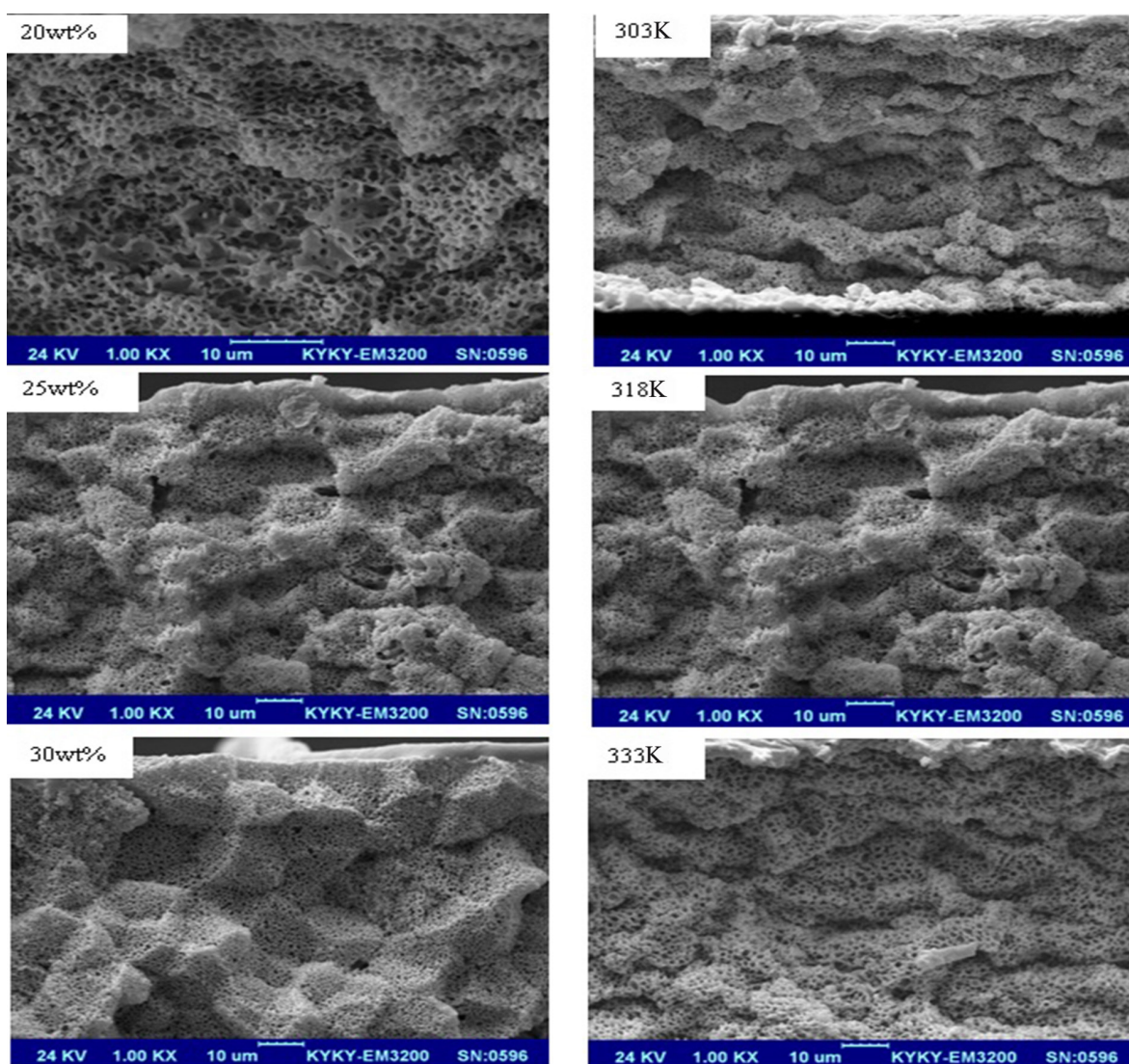
$$B > A > A^2 > AB > B^2$$

ANOVA can be used to make predictions about the response for given levels of each variable. Here, the prediction equation for each response is presented as follows:

$$\text{Porosity} = -266.55 - 7.02A + 2.1B - 1.75 \times 10^{-3}AB + 0.13A^2 - 2.33 \times 10^{-3}B^2$$

$$\text{Tensile} = 1.42 + 0.09A - 7.35 \times 10^{-3}B$$

$$\text{Flux} = 734.26 - 13.61A - 4.87B - 0.08AB + 0.67A^2 + 0.01B^2$$



(a) Temperature 318K

(b) Polymer concentration 25 wt%

Figure 7. Micrographs of cross-section of PP-g-MA membranes at (a) quenching bath temperature of 318 K and different concentrations (b) polymer concentration of 25wt% and different temperatures.

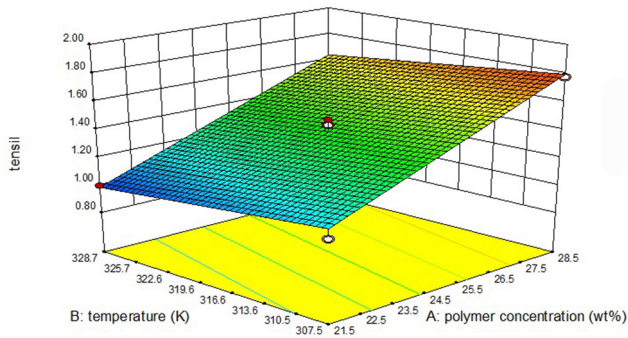


Figure 8. Effects of polymer concentration and bath temperature on membrane tensile.

Membrane performance

Porosity

For a more complete interpretation, we used a surface plot. A surface plot provides a three-dimensional view of how the variables affect the response. Figure 6 presents the effect of polymer concentration and quenching bath temperature on PP-g-MA membrane porosity. Due to decreasing the fraction of diluent-rich phase by increasing of the initial polymer concentration, the value of membrane porosity decreases [18]. At the fixed quenching bath temperature of 307 K and the polymer concentration of 21.5wt%, the value of porosity is 57.3%, while at the polymer concentration of 28.5wt%, the value of porosity is 49.7%. As shown in Figure 6, with increasing the bath temperature and subsequently decreasing the supercooling degree, the slower solidification rate of polymer-rich phase leaves longer time for polymer-lean phase to grow, so the final membrane pore size and porosity increase. This result is consistent with the SEM cross-sectional images (Figure 7).

Mechanical properties

The effect of polymer concentration and quenching bath temperature on PP-g-MA membrane mechanical properties was investigated and results are presented in Figure 8. The mechanical properties of the PP-g-MA membranes are increased by increasing the polymer concentration and decreasing the quenching bath temperature. As mentioned earlier in the PP-g-MA membrane preparation, the formation of droplets of the polymer-lean phase in the matrix of the polymer-rich phase and their growth determined the morphology and mechanical strength of the membrane. By increasing the initial polymer concentrations, the fraction of the polymer-lean phase is reduced and more compact membrane structure is formed, so the membrane tensile is increased. Figure 8 shows that by increasing the quenching bath temperature due to increasing the membrane porosity, tensile is decreased. As mentioned in the previous section, with increasing the bath temperature and solidification rate of polymer-rich phase, the final membrane pore size and porosity increase, and the tensile of membrane decreases.

Pure water flux

The values of pure water flux of PP-g-MA membranes at different polymer concentrations and quenching bath temperatures and at the pressure of 0.5 bar are presented in Figure 9. By decreasing the membrane pores size and porosities, due to increasing the initial PP-g-MA concentration, the water flowing resistance when water passes through the pores increases, so the pure water fluxes decreases. Increasing the membrane porosity decreases the resistance against pure water permeation, therefore by increasing the bath tempera-

Table 7. ANOVA of the regression model for pure water flux.

Source	Sum of Squares	df	Mean Square	F- Value	P-value Prob > F	
Model	8445.17	5	1689.03	42.22	< 0.0001	significant
A-polymer concentration	2840.68	1	2840.68	71.00	< 0.0001	
B-temperature	5075.41	1	5075.41	126.86	< 0.0001	
AB	35.66	1	35.66	0.89	0.3766	
A²	491.38	1	491.38	12.28	0.0099	
B²	18.55	1	18.55	0.46	0.5178	
Residual	280.06	7	40.01			not significant
Lack of Fit	42.56	3	14.19	0.24	0.8654	
Pure Error	237.51	4	59.38			
Cor Total	8725.23	12				
R² 0.9679	Adjusted R² 0.9450			Predicted R² 0.9228		

Table 8. Confirmation runs.

Run	A (wt%)	B (K)	Pure water flux(L/m ² h)			Porosity (%)			Tensile (MPa)		
			Actual	Predicted	Err (%)	Actual	Predicted	Err (%)	Actual	Predicted	Err (%)
1	21.5	307	101	100.21	-1.1	57.29	57.01	0.4	1.07	1.14	6.4
2	25	333	134	138.37	2.65	65.29	65.98	1.04	1.28	1.281	0.7
3	30	318	88	89.62	1.55	54.56	55.34	1.4	1.84	1.85	0.65
4	25.3	329	119	124.49	4.07	65.26	63.36	-3	1.31	1.34	2.16
5	26	313	78	83.68	6.38	55.9	53.87	3.8	1.48	1.52	2.51

Table 9. Optimal point in terms of the actual operating variables and output responses.

A (wt%)	B (K)	Pure water flux(L/m ² h)			Porosity (%)			Tensile (MPa)		
		Actual	Predicted	Err (%)	Actual	Predicted	Err (%)	Actual	Predicted	Err (%)
28.5	329	115.6	112.85	-2.4	62	61.2	-1.3	1.6	1.64	2.4

ture the pure water flux increases.

Validation runs and optimization

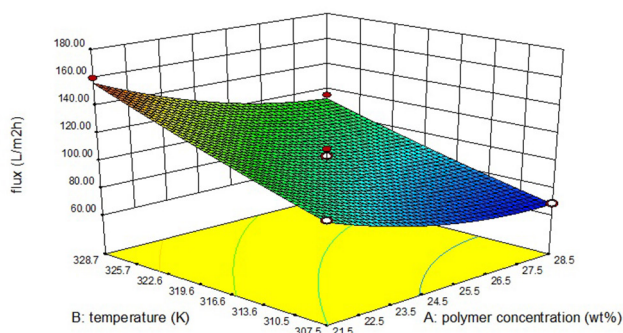
In order to predict the response of interest as a function of the variables at any polymer concentration and quenching bath temperature with the range of the levels defined, the regression equations obtained from the experimental data can be used. Five experimental points, three experiments (1–3) from the preparation conditions (Table 2) and two experiments (4–5) from new conditions within the defined limits of the variables, were selected to validate the veracity of the model (Table 8). As shown in Table 6, the actual experimental values and the predicted values were compared for the response of interest and the obtained results were reported. Calculated percentage errors indicated that the percentage errors for the flux, porosity and tensile changed from -1.1 to 6.38%, -3 to 3.8% and 0.7 to 6.4%, respectively. This results show that the regression models are acceptable and they can be used to predict and optimize the performance of the

PP-g-MA flat sheet membranes.

In order to achieve best responses (i.e. maximum flux, porosity and tensile values) optimization calculations have been carried out by using RSM methodology. The obtained results are presented in Table 9. Under the obtained optimal condition, the values of the flux, porosity and tensile are 115.6 L/m² h, 62% and 1.6 MPa, respectively. Comparison between the actual experimental values and the predicted values indicates that the regression models are suitable.

Comparison of a laboratory-made membrane with a commercial membrane

During the operation in the MBR, the transmembrane pressure (TMP), particle size distribution (PSD) and extracellular polymeric substance (EPS) of cake layer was measured under constant flow rate for a laboratory-made membrane and a commercial membrane (SINAP, flat sheet, size A4). In Table 10, the slope of TMP versus time is presented for the commercial membrane and laboratory-made membrane prepared under optimal condition. The obtained results reveal that the laboratory-made membrane is better than the commercial membrane. The membrane fouling for the laboratory-made membrane (TMP/Time = 0.3 kPa/d) was very slower than that for the commercial membrane (1.24 kPa/d). Also, the particle size distribution

**Figure 9.** Effects of polymer concentration and bath temperature on flux.**Table 10.** Slope of TMP versus time in the MBR system, PSD and mass value for cake layer on both membranes.

Membrane	TMP (kPa/d)	PSD (μ m)	Total cake (g/m ²)
Industrial	1.24±0.6	43.7±10.2	11.49
Experimental	0.3±0.12	65.4±8.3	3.6

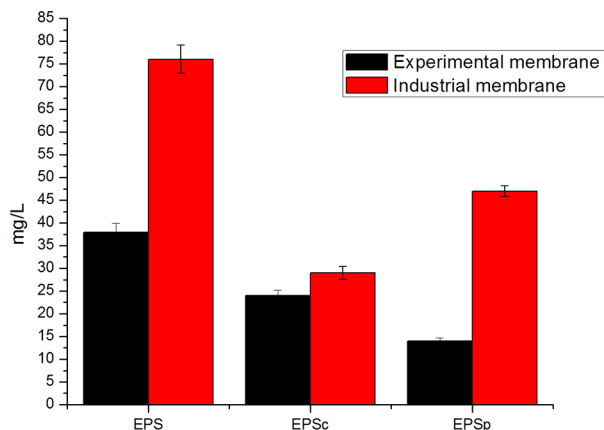


Figure 10. EPS concentration in the cake layer for both membranes.

of cake layer for both membranes has been shown in Table 10. The average particle size for cake layer at the end of operation with using the laboratory-made membrane (65.4 μm) is more than that with using the commercial membrane (43.7 μm). It is obvious that the larger particle on the laboratory-made membrane creates higher porosity and lower compressibility, causing less membrane fouling.

Figure 10 shows EPSp and EPSc in the cake layer for both membranes. EPSp and EPSc for cake layer in the laboratory-made membrane are lower than those in the commercial membrane. Due to higher EPS concentrations, especially EPSp, in the cake layer, the sticking tendency of the sludge to the membrane is higher for commercial membrane, which results in higher membrane fouling compared to laboratory-made membrane. The results show that total cake/bio-film on the membrane for laboratory-made membrane is lower than that for the commercial membrane. It might be due to higher hydrophilicity of laboratory-made membrane compared to commercial membrane.

CONCLUSION

In this study, with using the response surface methodology (RSM) based on the central composite design (CCD), PP-g-MA flat sheet membranes with using DOP/DBP mixture as a diluent were prepared by thermally-induced phase separation (TIPS). The ANOVA revealed that the bath temperature was the

most significant variable associated with porosity and pure water flux responses and the polymer concentration was the most significant variable associated with tensile response. The effects of polymer concentration and quenching bath temperature on morphology and performance of PP-g-MA membranes using CCD method were investigated. Further, comparison of laboratory-made membrane and commercial membrane was done in the MBR system. The following results were obtained:

- 1- By increasing the polymer concentration, the membrane porosity and pure water flux decreased, whereas the membrane mechanical properties increased.
- 2- By increasing the quenching bath temperature, the membrane porosity and pure water flux increased, whereas the membrane mechanical properties decreased.
- 3- According to the regression equations, the maximization responses were achieved under the following conditions: polymer concentration of 28.5 wt% and temperature of 329 K.
- 4- The membrane fouling occurred in a slower rate for laboratory-made membrane. The main reason for this slower rate is that, the EPS of cake layer for the laboratory-made membrane was lower than that for the commercial membrane.

REFERENCES

1. Jafarzadeh Y, Yegani R, Sedaghat M (2015) Preparation, characterization and fouling analysis of ZnO/polyethylene hybrid membranes for collagen separation. *Chem Eng Res Des* 94: 417-427
2. Lee MK, Lee J (2015) Mimicking permafrost formation for the preparation of porous polymer membranes. *Polymer* 74: 176-181
3. Cooney DA, Way JD, Wolden CA (2014) A comparison of the performance and stability of Pd/BCC metal composite membranes for hydrogen purification. *Inter J Hyd Energy* 39:19009-19017
4. Juang RS, Hou WT, Huang YC, Tseng YC, Huang C (2016) Surface hydrophilic modifications on polypropylene membranes by remote

- methane/oxygen mixture plasma discharges. *J Taiwan Ins Chem Eng* 65: 420–426
5. Gazagnes L, Cerneaux S, Persin M, Prouzet E, Larbot A (2007) Desalination of sodium chloride solutions and seawater with hydrophobic ceramic membranes. *Desalination* 217: 260-266
 6. Karkhanechi H, Rajabzadeh S, Nicolò ED, Usuda H, Matsuyama H, Preparation and characterization of ECTFE hollow fiber membranes via thermally induced phase separation (TIPS). *Polymer* 97: 515-524
 7. Tang YH, He YD, Wang XL (2015) Investigation on the membrane formation process of polymer–diluent system via thermally induced phase separation accompanied with mass transfer across the interface: Dissipative particle dynamics simulation and its experimental verification. *J Membr Sci* 474: 196-206
 8. Bang Ly H, Le Droumaguet B, Monchiet V, Grande D (2016) Tailoring doubly porous poly(2-hydroxyethyl methacrylate)-based materials via thermally induced phase separation. *Polymer* 86: 138-146
 9. Matsuyama H, Kim MK, Lloyd DR (2002) Effect of extraction and drying on the structure of microporous polyethylene membranes prepared via thermally induced phase separation. *J Membr Sci* 204: 413-419
 10. Madaeni SS, Rahimpour A (2005) Effect of type of solvent and non-solvents on morphology and performance of polysulfone and polyethersulfone ultrafiltration membranes for milk concentration. *Polym Adv Technol* 16: 717-724
 11. Liang HQ, Wu QY, Wan LS, Huang XJ, Xu ZK (2013) Polar polymer membranes via thermally induced phase separation using a universal crystallizable diluent. *J Membr Sci* 446: 482-493
 12. Krajewski SR (2006) Application of fluoroalkylsilanes (FAS) grafted ceramic membranes in membrane distillation process of NaCl solutions. *J Membr Sci* 281: 253-259
 13. Chou WL, Yang MC (2005) Effect of coagulant temperature and composition on surface morphology and mass transfer properties of cellulose acetate hollow fiber membranes. *Polym Adv Technol* 16: 524-532
 14. Sun X, Sun G, Wang X (2017) Morphology modeling for polymer monolith obtained by non-solvent-induced phase separation. *Polymer* 108: 432-441
 15. Buonomenna MG, Figoli A, Jansen JC, Drioli E (2004) Preparation of asymmetric PEEKWC flat membranes with different microstructures by wet phase inversion. *J Appl Polym Sci* 92: 576-591
 16. Zheng L, Wu Z, Zhang Y, Wei Y, Wang J (2016) Effect of non-solvent additives on the morphology, pore structure, and direct contact membrane distillation performance of PVDF-CTFE hydrophobic membranes. *J Environ Sci* 45: 28-39
 17. Wang Z, Yu W, Zhou C (2015) Preparation of polyethylene microporous membranes with high water permeability from thermally induced multiple phase transitions. *Polymer* 56: 535-544
 18. Luo B, Li Z, Zhang J, Wang X (2008) Formation of anisotropic microporous isotactic polypropylene (iPP) membrane via thermally induced phase separation. *Desalination* 233:19-31
 19. Jones TD, Chaffin KA, Bates FS (2002) Effect of tacticity on coil dimensions and thermodynamic properties of polypropylene. *Macromolecules* 35: 5061-5068
 20. Matsuyama H, Maki T, Teramoto M, Asano K (2002) Effect of polypropylene molecular weight on porous membrane formation by thermally induced phase separation. *J Membr Sci* 204: 323-328
 21. Lin Y, Chen G, Yang J, Wang X L (2009) Formation of isotactic polypropylene membranes with bicontinuous structure and good strength via thermally induced phase separation method. *Desalination* 236: 8-15
 22. Bae B, Chun BH, Kim D (2001) Surface characterization of microporous polypropylene membranes modified by plasma treatment. *Polymer* 42: 7879-7885
 23. Yu HY, Liu LQ, Tang ZQ, Yan MG, Gu JS, Wei XW (2008) Surface modification of polypropylene microporous membrane to improve its anti-fouling characteristics in an SBR: Air plasma treatment. *J Membr Sci* 311: 216-224
 24. Shi H, Shi D, Yin L, Luan S, Zhao J (2010) Syn-

- thesis of amphiphilic polycyclooctene-graft-poly (ethylene glycol) copolymers by ring-opening metathesis polymerization. *React Functional Polym* 70: 449-455
25. Saffar A, Carreau PJ, Kamal MR, Ajji A (2014) Hydrophilic modification of polypropylene microporous membranes by grafting TiO₂ nanoparticles with acrylic acid groups on the surface. *Polymer* 55: 6069-6075
 26. Wang H, Yang L, Zhao X, Yu T, Du Q (2009) Improvement of hydrophilicity and blood compatibility on polyethersulfone membrane by blending sulfonated polyethersulfone. *Chinese J Chem Eng* 17: 324-329
 27. Saffar A, Carreau PJ, Ajji A, Kamal MR (2014) Development of polypropylene microporous hydrophilic membranes by blending with PP-g-MA and PP-g-AA. *J Membr Sci* 462: 50-61
 28. Myers RH, Montgomery DC, Anderson-Cook CM (2009) *Response surface methodology: Process and product optimization using designed experiments*, New York, John Wiley & Sons.
 29. Wang C, Wei A, Wu H, Qu F, Chen W, Liang H, Li G (2016) Application of response surface methodology to the chemical cleaning process of ultrafiltration membrane. *Chinese J Chem Eng* 24: 651-657
 30. Ilbeygi HM, Ismail AF, Nasef MM, Jaafar J, Ghasemi M, Matsuura T, Zaidi SMJ (2014) Transport properties of SPEEK nanocomposite proton conducting membranes: Optimization of additives content by response surface methodology. *J Taiwan Ins Chem Eng* 45: 2265-2279
 31. Khayet M, Seman M, Hilal N (2010) Response surface modeling and optimization of composite nanofiltration modified membranes. *J Membr Sci* 349: 113-122
 32. Idris A, Kormin F, Noordin M (2006) Application of response surface methodology in describing the performance of thin film composite membrane. *Sep Purif Technol* 49: 271-280
 33. Wongkaew K, Wannachod T, Mohdee V, Pancharoen U, Arpornwichanop A, Lothongkum AW (2016) Mass transfer resistance and response surface methodology for separation of platinum (IV) across hollow fiber supported liquid membrane. *J Ind Eng Chem* 42: 23-35
 34. Subramonian S, Abdul Rahim S (2014) Comparison between Taguchi Method and Response Surface Methodology (RSM) in modelling CO₂ laser machining. *Jordan J Mechanical Ind Eng* 8: 35-42
 35. Fallon M, Walton AJ, Newsam MI, Gaston GJ (1995) A comparison of Taguchi methods and response surface methodology for optimising a CMOS process. *IEE Colloquium on Improving the Efficiency of IC Manufacturing Technology*, p. 4
 36. Luo F, Jun Z, Xiaolin W, Jianfei C, Zhongzi X (2002) Formation of hydrophilic ethylene-acrylic acid copolymer microporous membranes via thermally induced phase separation. *Acta Polym Sinica* 5: 566-571
 37. Chang IS, Lee CH, Ahn KH (1999) Membrane filtration characteristics in membrane coupled activated sludge system: The effect of floc structure on membrane fouling. *Sep Sci Technol* 34: 1743-1758
 38. Zhang XQ, Bishop PL, Kinkle BK (1999) Comparison of extraction methods for quantifying extracellular polymers in biofilms. *Water Sci Technol* 39: 211-218
 39. Dubois M, Gilles KA, Hamilton K, Rebers PA (1956) Colorimetric method for determination of sugars and related substances. *Anal Chem* 28: 350-357